Proceedings of the Korean Nuclear Society Spring Meeting
Kyungju, Korea, May 2003

The Correction Method of the Single Channel-Based CCP for the DUPIC Fuel

Park, J.W., Chae, K.M., Rhee, B.W., Choi, H., Yang, M.S.

Korea Atomic Energy Research Institute
P.O. Box 105, Yusong
Taejon, 305-600, Korea
E-mail:jwpark@kaeri.re.kr

Abstract

A thermal-hydraulic analysis of the DUPIC fuel loading in the CANDU reactor is presented. The CCP values obtained from the single channel analysis have been corrected for DUPIC fuel by comparing the CHF results of the 37-element and 43-element fuels of subchannel analysis. By sampling some important fuel channel, the CCP prediction uncertainty is quantified. It is found that the prediction uncertainty is not significantly large. This study shows that the axial power distribution of the DUPIC fuel bundle string may enhance the thermal margin. On the other hand the radial (ring) power distribution may degrade the thermal margin when compared with the standard fuel bundle string.

1. Introduction

A critical channel power (CCP) prediction technique for the DUPIC (Direct Use of spent PWR fuel In CANDU) fuel bundle in the CANDU reactor has been presented. The DUPIC fuel can be fabricated[1] remotely from the spent PWR fuel, that is, through the nuclear proliferation-resistant dry-reprocessing process[2]. The 43-element fuel bundle has been chosen as the DUPIC fuel carrier in this study.

The CANDU reactor core has been designed by the single channel analysis. In the single channel analysis, the coolant flow passage in a fuel channel can be simplified as a straight pipe of equivalent diameter. The pressure boundary condition is normally used by assuming that the inlet and outlet header pressures are fixed. Additionally, every fuel channel is assumed to have no dynamic communication between each other.

The CCP prediction technique requires experimentally validated CHF correlation which can be consistently used in the single channel analysis. Unfortunately, however, it is impossible to run the experiment for all the flow and thermal boundary conditions since the real-scale CHF experiment is quite expensive. Therefore, a finite amount of the experimental data needs to be interpolated (or, sometimes, extrapolated) when applied to a specified flow condition in the single channel analysis[3]. This type of design analysis methodology requires independent sets of experimental data for new

type of fuel (e.g., 43-element fuel) of which the geometry and the radial power distribution is quite different from the conventional fuel bundle. A correlation for 43-element fuel was generated[4] and the validity of this correlation for wider range of thermophysical condition is of interest.

On the other hand, the subchannel analysis was developed with the aim of simulating the effect of multi-dimensional flow phenomena which occur in various fuel bundle geometries[6]. Through the lateral flow model, the radial geometry of the fuel bundle can be efficiently taken into account. Nevertheless, the subchannel analysis has not been adopted as the fuel design analysis for the heavy water reactor yet. One of important reasons for this is that the subchannel analysis may not improve predicting accuracy of CHF in 37-element bundle strings enough to substitute the existing design practice of the single channel analysis. It is obvious, however, that the effect of the radial flow distribution within a fuel bundle cannot be mechanistically simulated by the single channel code which has no radial flow model. Due to this reason, the effect of the ring power distribution (the radial power distribution) inside a fuel bundle cannot be reasonably described by single channel model. Moreover, the radial geometry change of the 43-element fuel bundle over the 37-element fuel can be properly simulated by the subchannel code.

In this study, the combined effect of the power distribution and the radial bundle geometry of the 43-element DUPIC fuel have been investigated. The effect of the axial power distribution on the CCP has been quantified by using the single channel analysis while the effect of radial geometry on CCP has been taken into account by subchannel analysis. The results include the critical channel power, the critical power ratio, and the channel flow for the DUPIC fuel and the 37-element natural uranium fuel.

2. The CCP Correction Method

The effect of the difference of the radial geometry and the ring power distribution has been quantified by using the subchannel analysis code. The assumption used in this study is that the effects of the radial and axial power to the dryout phenomenon can be decoupled. Using this assumption, one may correct the CCP values (i.e., CCP_{DUPIC}^{NUCIRC}) calculated by the NUCIRC code (the single channel model) as:

$$CCP_{DUPIC} = CCP_{DUPIC}^{NUCIRC} \times F_R \quad (1)$$

where F_R is the radial correction factor induced by approximating the power and the bundle shape of the DUPIC fuel to those of the standard fuel in the single channel calculation. To isolate the effect of radial flow distribution, ASSERT-PV was used to evaluate CCPs for both of the fuel types using the same axial power shape. That is, the radial correction factor was obtained from the result of the subchannel analysis as:

$$F_R = \frac{CCP_{DUPIC}^{ASSERT}}{CCP_{NU}^{ASSERT}} \quad (2)$$

The unique radial correction factor may exist for every fuel channel. It is, however,

not reasonable to evaluate F_R for every fuel channel since it requires formidably large amount of calculations. Therefore, instead, the idea used in this study is the stochastic technique in which we may evaluate mean value of the radial correction factors for the *representative* channels and apply this value for all of the similar fuel channels. The cost of this method is an increase of the CCP prediction uncertainty. The representative channels are selected as in Table 1 along with its channel characteristics. By using the ASSERT-PV code, the radial correction factor has been obtained as in Table 2. As can be seen, the radial correction factors are consistently less than 1.0 that means the thermal margin should be slightly reduced due to the radial geometry effect of the DUPIC fuel bundle. The mean value of the radial correction factor, however, turned out to be very close to unity (i.e., F_R = 0.9907) and the standard deviation of the radial correction factor is less than 1% as shown in Table 2. This result suggests that the effect of the radial geometry of the DUPIC fuel in CCP prediction is very small. The uncertainty in the CCP prediction should be slightly increased due to the radial correction as:

$$\Delta_{DUPIC}^{CCP} = \Delta_{NU}^{CCP} + \Delta_{DUPIC}^{F_R} \tag{3}$$

where

$$\Delta_{DUPIC}^{F_R} = 0.93\% \tag{3a}$$

The uncertainty incurred from this method should be added to the uncertainty of existing CCP prediction. It will be shown shortly that the sole disadvantage in the thermal margin of the DUPIC fuel is the increase of the CCP prediction uncertainty since the minimum CPR of DUPIC core is higher than that of the standard core. It should be noted that the uncertainty given by Eq.(3a) is no negligible amount per thermal design experience.

3. Results and Discussion

The important input of the CCP analysis is the axial power distribution of the fuel channel. The axial power distribution of the core loaded with the conventional fuel bundle string is close to a chopped cosine shape which is almost symmetric in the axial direction. The symmetric axial power distribution can be retained as far as the excess reactivity of each fuel bundle is the same as that of the 37-element bundle of natural uranium fuel. The axial power distribution can be skewed toward the fuel channel inlet if the amount of the excess reactivity of the fresh fuel bundle is increased. In general, the eight (8) bundle shift refueling can not be used for fuel of higher enrichment than the natural uranium. Instead, two or four bundle shifts is known to be inevitable because the reactor overall reactivity needs to be controlled. The four bundle shift was assumed in this analysis. Even though there is a neutron flux smoothening effect between interlaced neighboring fuel channels, higher enrichment fuel loading may result in good

axial power skew. The inlet-skewed axial power distribution normally changes thermal-hydraulic characteristics of the fuel channel. As a result, the critical channel power can be affected.

Thermal-hydraulic parameters of the fuel channels of CANDU reactor loaded by either the standard or the DUPIC fuel bundles are presented at 100% of reactor full power. The characteristics of DUPIC fuel bundle strings can be reasonably understood at 100% power condition since no dramatically different thermal behaviors are expected under other operating conditions.

The feeder and orifice geometry data of the existing CANDU reactor design (i.e., Wolsong 2 reactor) have been used in this analysis. Due to different pressure drop characteristics in the fuel channel induced by the different channel power distributions and the shape of the fuel bundle, the coolant flow rate of each fuel channel was changed and therefore new heat balance for the DUPIC fuel bundle string can be established.

The channel power distribution for the DUPIC and the standard fuel was obtained from the neutron physics calculation. As shown in Fig.1, the axial power shape of the DUPIC fuel is known to be inlet-skewed when compared with that of the standard fuel. The axial power distribution of the channel L11, which has minimum critical power ratio and was selected as the representative channel, for the DUPIC and the standard fuels are compared in Fig.1. As can be seen, the axial power distribution of the DUPIC fuel is inlet-skewed and the other peak at the down stream is due to the refueling effect of the surrounding fuel channels. It should be noted that in general the inlet peak is known to increase the CHF margin while the exit peak does not.

The radial power shape of the DUPIC core was found to be very similar to that of the standard core. In fact, the radial power peak of the DUPIC core is slightly higher than the standard core.

Using the header-to-header pressure drop, the reactor inlet header temperature and the reactor outlet header pressure as the boundary conditions, the power to channel flow ratio distributions have been obtained as shown in Figs. 2 and 3. As can be seen, no much difference can be found against the radial distance from the core center.

It should be noted that the total flow used in this study is quite low if compared with the Wolsong' s commissioning test value of 8689 kg/s[9]. The difference between the design value and the commissioning test value is normally quite large if the measured values from the plant are not fed back to modify the thermophysical input values.

The corrected critical channel powers for the standard and the DUPIC fuels are shown in Fig. 5. In the CCP calculations, the axial power distribution is an important input and it is quite different from each other for the standard and the DUPIC fuels. As can be seen in Fig.5, the maximum value of CCP is slightly higher in the DUPIC core. The location of the maximum CCP which are both in the central region where the channel power is high, show that thermal performance of these fuel would be very similar.

The critical power ratio (CPR) is the ratio of the critical channel power to the actual channel power, which is the direct measure of thermal margin of the fuel channel. It should be noted, however, that the CPR is not linearly proportional to the thermal margin[1]. As shown in Fig. 5, the minimum CPR in the DUPIC core is found to be 1.414 at H07 channel in the DUPIC core, while it is 1.365 at O06 channel for the standard core. This result shows that the worst thermal condition (i.e., the least thermal margin) may occur in the periphery of the high power region for both fuels. The

minimum CPR value does not hit 1.12, which is the design requirement for CPR.

4. Conclusion

The Critical Channel Power of the DUPIC core in the CANDU reactor has been predicted. It is found from the result of the single channel code calculations that there is no significant difference between thermal-hydraulic behaviors of the DUPIC and the standard fuel bundles. Based upon the result of the critical power ratio, the DUPIC fuel bundle strings in the CANDU reactor turned out to slightly increase the reactor thermal margin when the radial correction factor is neglected. The result of subchannel analysis was used for validating the CCP model for the DUPIC fuel bundle since the same dryout model was used for CCP evaluation. The radial geometry effect of the DUPIC fuel has been taken into account by using the radial correction factor evaluated from the subchannel analysis. It is found that there is no significant difference in the dryout power. The dryout locations are also very similar for the two fuel bundles. It was found, however, that the radial (ring) power distribution is very important for the void distribution in the fuel. Based upon the subchannel analysis, it has been found that the uncertainty induced by using the same dryout correlation (the x_c-L_b correlation) for the DUPIC fuel is small. The result of the subchannel analysis suggests that the CCP value of the DUPIC fuel should be reduced by factor of 0.9907 and additional uncertainty of 0.93% may need to be added in the CCP prediction for the DUPIC fuel bundle. If we recall the CCP values of the DUPIC fuel evaluated by the NUCIRC code are slightly higher than those of the standard fuel, there should not be much difference in the actual CCP values between the two fuel types.

This study revealed that the DUPIC fuel be used for CANDU reactor without losing much thermal margin

Acknowledgements

This work was supported by Nuclear Mid-Long Term Research Fund of Korea Ministry of Science and Technology.

References

1. Kang, K.H., Ryu, H.J., Song, K.C. and Yang, M.S., 2002, "Thermal expansion of UO_2 and simulated DUPIC fuel", J. Nuclear Materials, 301.
2. Yang, M.S. and Gadsby, R., 2001, "DUPIC Fuel Cycle", Encyclopedia of Materials: Science and Technology, pp. 2368-2370
3. Groeneveld, D.C., 1996, “On the Definition of Critical Heat Flux Margin”, Nuclear Eng. Des., 163.
4. Leung, L.K.H and Groeneveld, D.C., 1991, “A Method for Predicting Critical Heat Flux of a String of CANFLEX Bundle”, ARD-TD-304.
5. Carver, M.B., Kiteley, J.C., Zhou, R.Q.N., Junop, S.V. and Rowe, D.S., 1995, “Validation of the ASSERT Subchannel Code: Prediction of Critical Heat Flux in Standard and Nonstandard CANDU Bundle Geometries”, Nuclear Technology, 112.
6. Tapucu, A., Teyssedou, A., Tye, P. and Troche, N., 1994, “The Effect of Turbulent

Mixing Models on the Prediction of Subchannel Codes", Nuclear Eng. Des., 149.
7. Lahey, R.T., Jr. and Moody, F.J., 1993, "The Thermal-Hydraulics of A Boiling Water Reactor", 2nd Edition, ANS Monograph.
8. Park, J.-W. 1998, "A Subchannel Analysis of the DUPIC Fuel Bundle in CANDU Reactor", Annals of Nuclear Energy, 26.
9. Harvel, G.D., 1998, "Wolsong 3,4, PHT System Flow Verification Procedure", AECL-TD-86-33100-610-001.

Table 2. Selected Fuel Channels for the Radial Correction Factor Calculation

Channel Flow (Kg/s)		Fuel Channel Conditions
DUPIC	Standard	
24.23 (H07)	24.94 (O06)	Minimum CPR channel
26.73 (L05)	27.20 (L05)	Maximum channel flow
25.20 (P08)	26.80 (M05)	Maximum channel power
11.63 (A14)	11.71 (A09)	Maximum channel exit quality
24.33 (N04)	24.63 (N04)	Maximum fuel element temperature*

Table 3. Radial Correction Factor

Fuel Channel	Channel Flow (kg/s)	Critical Channel Power (kw)		Radial Correction Factor (F_R)
		CCP_{NU}	CCP_{DUPIC}	
A09	11.71	6950	6790	0.9770
A14	11.63	6920	6750	0.9754
H07	24.23	11220	11150	0.9938
L05	26.97	12200	12190	0.9992
M05	26.80	12140	12120	0.9984
N04	24.48	11310	11250	0.9947
O06	24.94	11500	11410	0.9922
P08	25.20	11310	11250	0.9947
Mean Value				0.9907
Standard Deviation				0.009236 (0.93%)

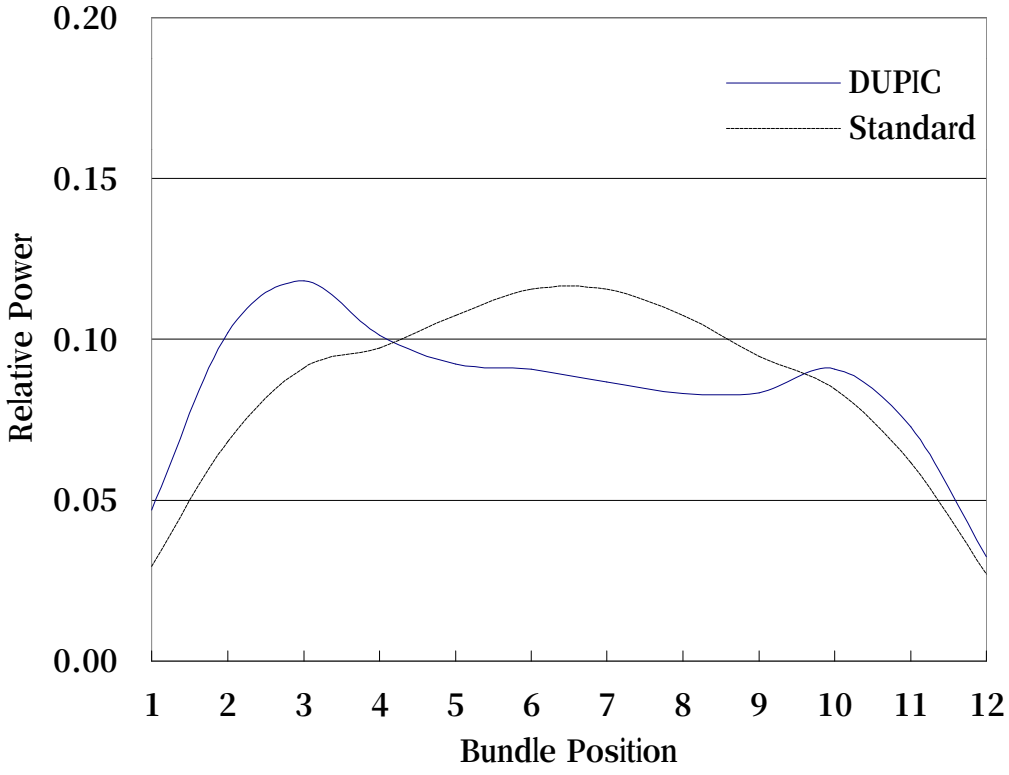

Figure 1. Axial Power Distribution of DUPIC and Standard Fuel for Channel L11 at 100% F.P. Normal Operating Condition

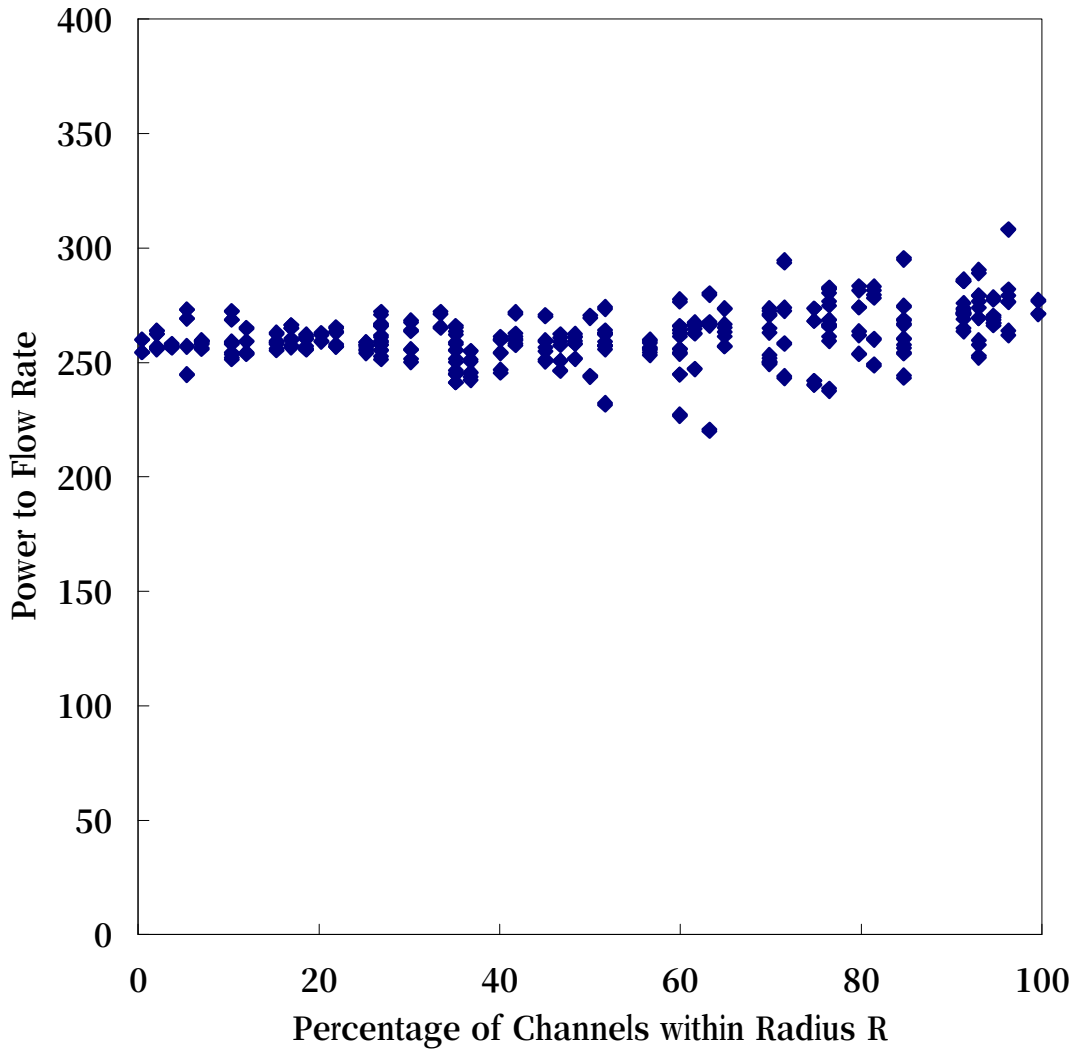

Figure 2. Power to Flow Ratio of DUPIC Fuel

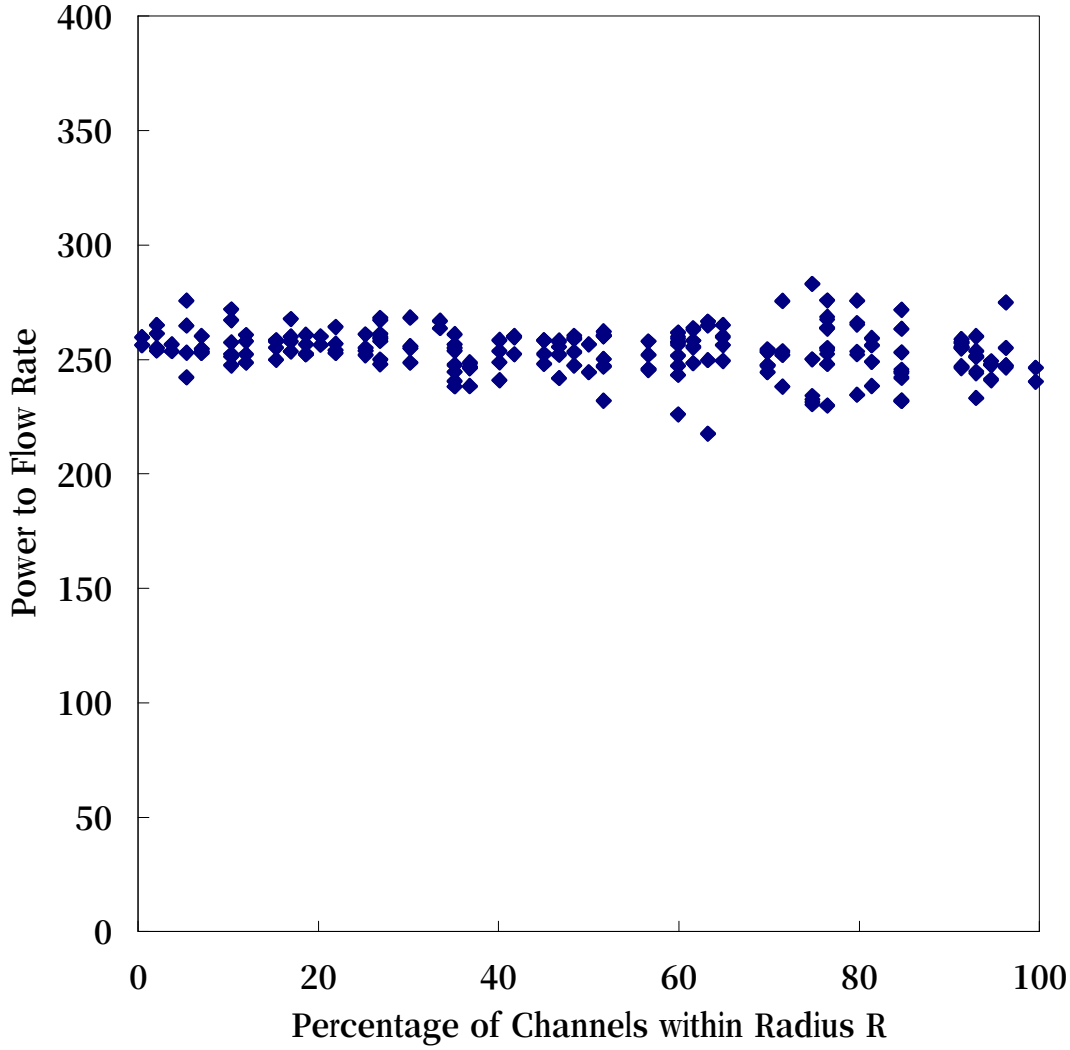

Figure 3. Power to Flow Ratio of Standard (NU) Fuel

	1	2	3	4	5	6	7	8	9	10	11	12	13	14	15	16	17	18	19	20	21	22
A									5318	5675	5695	5696	5675	5318								
B						5223	5708	6797	7184	7186	7223	7222	7187	7184	6800	5707	5223					
C					5563	6123	7019	7571	7777	8167	8218	8218	8166	7777	7570	7018	6119	5564				
D				5606	6508	7166	7787	8529	8738	8841	8833	8832	8841	8737	8529	7789	7167	6507	5608			
E			5857	6453	7434	8030	8499	8817	9022	9081	9229	9230	9081	9022	8817	8504	8027	7435	6449	5858		
F			6550	7347	8172	8552	8864	9081	9045	9121	9060	9058	9122	9044	9082	8862	8553	8170	7349	6548		
G		6063	7067	7861	8533	8855	8912	9069	9087	9109	9140	9142	9107	9089	9068	8913	8856	8533	7859	7071	6063	
H		6669	7674	8532	8809	8941	8955	9122	9105	9069	9055	9054	9073	9105	9123	8955	8942	8808	8533	7679	6673	
J	5489	6899	8093	8771	9142	9175	9222	9295	9251	9229	9093	9093	9229	9251	9294	9221	9174	9143	8773	8095	6899	5495
K	5712	7147	8268	8969	9249	9171	9234	9294	9232	9195	9085	9084	9196	9232	9294	9233	9174	9245	8973	8267	7149	5714
L	6100	7682	8444	9163	9410	9266	9366	9422	9291	9166	8923	8923	9167	9287	9420	9365	9266	9413	9163	8444	7683	6106
M	6091	7639	8428	9051	9345	9364	9337	9375	9423	9162	9066	9064	9162	9424	9373	9341	9363	9346	9050	8432	7640	6096
N	6000	7271	8271	8953	9309	9216	9242	9408	9253	9174	8995	8994	9175	9251	9409	9241	9217	9308	8954	8269	7271	6001
O	5799	6990	8013	8736	9084	9097	9177	9266	9232	9164	8969	8971	9163	9233	9268	9178	9096	9085	8735	8014	6989	5802
P		6767	7964	8523	8869	9062	9088	9245	9209	9165	9035	9034	9166	9207	9246	9087	9067	8867	8523	7963	6771	
Q		6069	7316	8480	8721	8877	8941	9153	9169	9224	9099	9101	9222	9170	9155	8943	8875	8725	8479	7322	6065	
R			6698	7509	8300	8653	8841	9127	9149	9136	9111	9109	9138	9148	9128	8839	8655	8296	7512	6695		
S			5554	6666	7379	8023	8515	8869	9136	9385	9321	9322	9385	9138	8868	8517	8021	7380	6665	5558		
T				5748	6496	7248	7828	8437	8746	8843	8841	8841	8843	8746	8438	7828	7249	6496	5749			
U					5375	6018	6892	7824	7926	8237	8224	8221	8237	7927	7823	6893	6018	5376				
V						4989	5691	6496	6614	6845	6838	6838	6845	6613	6496	5691	4990					
W									5499	5635	5858	5858	5635	5500								

Standard Fuel (NU)

	1	2	3	4	5	6	7	8	9	10	11	12	13	14	15	16	17	18	19	20	21	22
A									5519	5845	5875	5875	5845	5520								
B						5426	5877	6989	7322	7351	7376	7375	7352	7323	6989	5876	5427					
C					5768	6275	7206	7690	7895	8255	8305	8305	8254	7895	7690	7207	6275	5769				
D				5819	6653	7340	7899	8629	8807	8907	8887	8886	8908	8806	8630	7898	7341	6652	5821			
E			6068	6607	7591	8127	8598	8894	9081	9120	9250	9251	9119	9081	8894	8599	8123	7593	6606	6069		
F			6728	7507	8257	8640	8937	9137	9100	9160	9103	9101	9162	9098	9138	8936	8642	8255	7509	6727		
G		6255	7241	7965	8613	8910	8990	9123	9142	9152	9197	9198	9150	9143	9122	8991	8910	8617	7965	7240	6254	
H		6862	7804	8611	8864	8987	9014	9175	9155	9124	9123	9123	9125	9154	9176	9014	8987	8861	8613	7804	6863	
J	5684	7067	8200	8836	9175	9201	9260	9330	9297	9275	9154	9154	9275	9297	9330	9260	9202	9175	8836	8204	7068	5686
K	5891	7314	8358	9039	9270	9208	9270	9332	9278	9239	9138	9138	9240	9278	9332	9270	9206	9271	9040	8360	7318	5893
L	6303	7802	8535	9226	9439	9309	9404	9452	9335	9217	8977	8978	9217	9335	9452	9404	9309	9439	9225	8537	7804	6305
M	6293	7763	8525	9118	9385	9410	9385	9414	9457	9213	9114	9115	9213	9453	9410	9385	9410	9386	9117	8527	7763	6295
N	6190	7426	8372	9024	9352	9273	9292	9449	9299	9222	9051	9050	9223	9298	9447	9292	9274	9351	9026	8373	7428	6191
O	6011	7154	8131	8814	9148	9161	9235	9316	9283	9217	9043	9044	9216	9284	9315	9237	9160	9149	8813	8135	7153	6013
P		6960	8095	8610	8928	9114	9152	9301	9258	9219	9106	9105	9220	9256	9302	9152	9115	8927	8612	8094	6962	
Q		6267	7476	8563	8819	8941	9022	9212	9223	9272	9162	9164	9270	9224	9211	9024	8939	8821	8560	7481	6266	
R			6884	7668	8426	8730	8913	9187	9204	9192	9164	9162	9193	9203	9188	8912	8733	8423	7670	6882		
S			5755	6822	7570	8117	8608	8938	9197	9414	9342	9343	9413	9198	8936	8609	8112	7571	6821	5757		
T				5939	6639	7405	7933	8530	8817	8903	8894	8893	8904	8817	8530	7932	7406	6638	5940			
U					5549	6155	7055	7925	8030	8309	8305	8306	8308	8031	7925	7056	6154	5549				
V						5133	5808	6645	6731	6984	6970	6969	6985	6730	6646	5807	5134					
W									5594	5728	5979	5979	5728	5595								

DUPIC Fuel

Figure 4. Critical Channel Power Distributions

	1	2	3	4	5	6	7	8	9	10	11	12	13	14	15	16	17	18	19	20	21	22
A									1.562	1.616	1.587	1.589	1.618	1.566								
B						1.671	1.555	1.639	1.629	1.572	1.569	1.570	1.575	1.634	1.646	1.563	1.681					
C					1.603	1.505	1.507	1.487	1.451	1.493	1.518	1.519	1.496	1.456	1.493	1.515	1.514	1.617				
D				1.555	1.519	1.449	1.418	1.457	1.445	1.451	1.479	1.480	1.454	1.449	1.464	1.427	1.460	1.532	1.572			
E			1.679	1.501	1.489	1.438	1.409	1.401	1.417	1.430	1.482	1.483	1.433	1.422	1.408	1.419	1.449	1.504	1.518	1.705		
F			1.566	1.481	1.477	1.422	1.394	1.396	1.416	1.441	1.443	1.443	1.444	1.421	1.404	1.403	1.434	1.492	1.500	1.591		
G		1.590	1.500	1.439	1.459	1.425	1.379	1.387	1.415	1.429	1.426	1.427	1.432	1.421	1.394	1.389	1.438	1.476	1.457	1.525	1.623	
H		1.556	1.478	1.456	1.443	1.408	1.377	1.396	1.417	1.421	1.410	1.411	1.425	1.423	1.404	1.388	1.422	1.460	1.476	1.503	1.588	
J	1.566	1.498	1.459	1.427	1.458	1.440	1.429	1.440	1.448	1.457	1.439	1.440	1.460	1.454	1.448	1.440	1.454	1.475	1.447	1.483	1.527	1.608
K	1.534	1.463	1.423	1.409	1.442	1.425	1.429	1.445	1.454	1.467	1.469	1.470	1.471	1.460	1.454	1.440	1.440	1.458	1.429	1.445	1.492	1.573
L	1.582	1.528	1.417	1.404	1.417	1.399	1.434	1.462	1.467	1.476	1.472	1.473	1.480	1.473	1.470	1.445	1.412	1.434	1.423	1.439	1.557	1.622
M	1.587	1.520	1.410	1.376	1.388	1.394	1.417	1.449	1.486	1.476	1.500	1.501	1.480	1.492	1.457	1.428	1.407	1.403	1.394	1.431	1.548	1.625
N	1.637	1.495	1.416	1.381	1.388	1.369	1.398	1.448	1.453	1.467	1.469	1.470	1.471	1.458	1.456	1.408	1.381	1.402	1.398	1.436	1.521	1.673
O	1.683	1.524	1.437	1.395	1.383	1.365	1.388	1.420	1.443	1.450	1.423	1.425	1.453	1.448	1.427	1.398	1.376	1.397	1.411	1.458	1.550	1.721
P		1.603	1.549	1.458	1.443	1.415	1.390	1.413	1.440	1.444	1.411	1.412	1.447	1.445	1.420	1.398	1.427	1.456	1.475	1.571	1.632	
Q		1.637	1.601	1.601	1.539	1.469	1.414	1.425	1.449	1.464	1.430	1.432	1.467	1.454	1.432	1.423	1.479	1.554	1.618	1.624	1.665	
R			1.698	1.618	1.627	1.546	1.462	1.457	1.471	1.471	1.467	1.468	1.474	1.475	1.464	1.470	1.557	1.640	1.636	1.720		
S			1.740	1.711	1.657	1.588	1.516	1.489	1.496	1.531	1.550	1.552	1.533	1.501	1.495	1.524	1.598	1.670	1.727	1.762		
T				1.843	1.741	1.658	1.586	1.581	1.571	1.568	1.598	1.599	1.571	1.575	1.587	1.593	1.668	1.753	1.859			
U					1.885	1.750	1.719	1.760	1.677	1.697	1.714	1.714	1.700	1.681	1.766	1.727	1.759	1.898				
V						2.086	1.944	1.917	1.804	1.782	1.756	1.757	1.785	1.809	1.924	1.952	2.097					
W									2.171	2.092	2.101	2.102	2.095	2.176								

Standard Fuel (NU)

	1	2	3	4	5	6	7	8	9	10	11	12	13	14	15	16	17	18	19	20	21	22
A									1.572	1.630	1.605	1.605	1.631	1.573								
B						1.701	1.582	1.666	1.648	1.598	1.593	1.593	1.599	1.650	1.668	1.584	1.705					
C					1.639	1.540	1.547	1.511	1.474	1.509	1.532	1.532	1.510	1.475	1.513	1.550	1.543	1.644				
D				1.597	1.556	1.492	1.447	1.481	1.462	1.466	1.491	1.491	1.467	1.464	1.484	1.450	1.495	1.561	1.603			
E			1.722	1.544	1.533	1.470	1.439	1.424	1.432	1.440	1.491	1.491	1.441	1.434	1.427	1.442	1.473	1.538	1.550	1.731		
F			1.611	1.529	1.511	1.455	1.424	1.419	1.436	1.456	1.470	1.470	1.458	1.438	1.421	1.427	1.459	1.516	1.535	1.618		
G		1.634	1.555	1.480	1.495	1.456	1.420	1.418	1.434	1.444	1.454	1.455	1.445	1.436	1.421	1.424	1.460	1.501	1.486	1.563	1.644	
H		1.614	1.530	1.499	1.479	1.440	1.414	1.424	1.433	1.434	1.435	1.435	1.436	1.434	1.427	1.418	1.444	1.484	1.506	1.538	1.624	
J	1.629	1.565	1.514	1.473	1.497	1.483	1.459	1.460	1.461	1.466	1.452	1.453	1.467	1.463	1.462	1.463	1.488	1.503	1.480	1.522	1.574	1.642
K	1.610	1.537	1.481	1.462	1.491	1.478	1.460	1.465	1.466	1.474	1.478	1.478	1.475	1.467	1.468	1.464	1.483	1.497	1.469	1.488	1.547	1.623
L	1.671	1.602	1.482	1.463	1.475	1.459	1.470	1.483	1.480	1.484	1.480	1.481	1.485	1.482	1.485	1.473	1.463	1.480	1.469	1.489	1.611	1.683
M	1.685	1.604	1.486	1.445	1.457	1.462	1.461	1.476	1.502	1.490	1.512	1.513	1.490	1.504	1.478	1.464	1.466	1.461	1.450	1.492	1.613	1.697
N	1.736	1.586	1.495	1.453	1.458	1.440	1.445	1.479	1.474	1.483	1.486	1.486	1.485	1.476	1.481	1.447	1.442	1.462	1.458	1.501	1.595	1.747
O	1.779	1.616	1.518	1.466	1.449	1.430	1.439	1.456	1.467	1.469	1.450	1.450	1.470	1.468	1.458	1.441	1.433	1.453	1.471	1.525	1.623	1.790
P		1.688	1.628	1.525	1.500	1.465	1.441	1.453	1.462	1.463	1.445	1.445	1.464	1.464	1.455	1.443	1.468	1.503	1.530	1.634	1.696	
Q		1.703	1.673	1.656	1.590	1.508	1.459	1.458	1.466	1.477	1.457	1.458	1.477	1.468	1.459	1.461	1.511	1.594	1.660	1.680	1.711	
R			1.749	1.666	1.662	1.568	1.480	1.467	1.476	1.473	1.478	1.478	1.474	1.477	1.469	1.482	1.571	1.665	1.671	1.754		
S			1.760	1.725	1.673	1.582	1.509	1.475	1.477	1.504	1.521	1.521	1.504	1.479	1.477	1.511	1.584	1.676	1.728	1.766		
T				1.788	1.694	1.620	1.541	1.534	1.520	1.514	1.539	1.540	1.515	1.520	1.535	1.543	1.623	1.697	1.792			
U					1.734	1.634	1.620	1.648	1.575	1.590	1.605	1.605	1.590	1.576	1.650	1.622	1.636	1.737				
V						1.768	1.691	1.696	1.611	1.606	1.584	1.584	1.607	1.612	1.697	1.693	1.771					
W									1.718	1.708	1.737	1.737	1.708	1.719								

DUPIC Fuel

Figure 5. Critical Power Ratio Distributions